Tunneling spectroscopy study of YBa$_2$Cu$_3$O$_7$ thin films using a cryogenic scanning tunneling microscope

R. Wilkins and M. Amman

Department of Physics, The University of Michigan, Ann Arbor, Michigan 48109

R. E. Soltis

Scientific Laboratory, The Ford Motor Company, Dearborn, Michigan 48121

E. Ben-Jacob*

*Department of Physics, The University of Michigan, Ann Arbor, Michigan 48109
and Scientific Laboratory, The Ford Motor Company, Dearborn, Michigan 48121*

R. C. Jaklevic

Scientific Laboratory, The Ford Motor Company, Dearborn, Michigan 48121

We have measured reproducible tunneling spectra on YBa$_2$Cu$_3$O$_7$ ($T_c \sim 85$ K) thin films (thickness ~ 2 μm) with a cryogenic scanning tunneling microscope. We find that the I-V curves are generally of three types. The most common type, featured in a large majority of the data, shows a region of high conductance at zero bias. The amplitude of this region is inversely proportional to the tunneling resistance between the tip and sample. It is possible that this can be explained in terms of Josephson effects within the films, although an alternative is given based on electronic self-energy corrections. Data showing capacitive charging steps are analyzed in terms of two ultrasmall tunnel junctions in series.. Theoretical fits to the data give specific values of the junction parameters that are consistent with the assumed geometry of the tip probing an individual grain of the film. The third type of I-V curves exhibits negative differential resistance. We conclude that this phenomenon is probably due to tunneling to localized states in the surface oxide. We also present and discuss data with energy-gap-like behavior; the best example gives Δ to be about 27 mV.

I. INTRODUCTION

In 1987 superconductivity was found to exist in certain copper oxide ceramic materials at temperatures above 77 K. Researchers worldwide have employed a great variety of experimental tools to probe the nature of these materials. One of the tools that has traditionally been used to study the electronic structure and coupling mechanism of superconductors has been tunneling spectroscopy. Specifically, the superconducting energy gap Δ, phonon density of states, and magnitude of the electron-phonon coupling have been deduced for many classes of superconductors using tunneling spectroscopy.[1] Similar measurements were attempted on the new oxides. Unfortunately, the initial studies (for example, Refs. 2 and 3), using point contact junctions, reported difficulty measuring the gap or even identifying consistent features in the I-V curves. Complicating these experiments is a relatively thick, nonsuperconducting surface oxide layer characteristic of these ceramics when exposed to air. In addition, these materials have short coherence lengths which make it difficult to probe the electronic structure of the crystal. Various methods[4−6] have been used to overcome these problems. However, only recently[7] have reproducible single electron tunneling data been obtained that convincingly reflect the properties of the YBa$_2$Cu$_3$O$_7$ single crystal. The crystals were cleaned by chemical etching and treated in air to develop a controlled tunneling barrier.

In this paper, we show reproducible data obtained from point contact junctions formed between the tip of a cryogenic scanning tunneling microscope (CSTM) and thin films of YBa$_2$Cu$_3$O$_7$. No attempt has been made to remove or reduce the surface oxide layer. In fact, this layer may be responsible for some of the effects observed. Understanding the effects of the oxide layer on the electrical properties of these ceramics is important for possible technological applications of these materials. For example, given the thickness and toughness of this layer, simply making reliable electrical contact to the material presents a challenge.

II. EXPERIMENT

The Y-Ba-Cu-O films were deposited on (10$\bar{1}$0) sapphire by sputtering from a single target using a magnetically enhanced rf triode sputter source.[8] The target was prepared by hot pressing at 900 °C and 8000 psi unreacted Y$_2$O$_3$, BaCO$_3$, and CuO powders in proportion corresponding to the stoichiometric YBa$_2$Cu$_3$O$_7$ composition. The powders remained essentially unreacted, but were highly compacted with less than 5% porosity. Argon with 1–3% oxygen was used as the sputtering gas at a pressure in the range of 1–10 mTorr. The sapphire substrates were resistively heated during deposition up to 450 °C. The deposition rate was of the order of 100 Å/min. The as deposited films were black but amor-
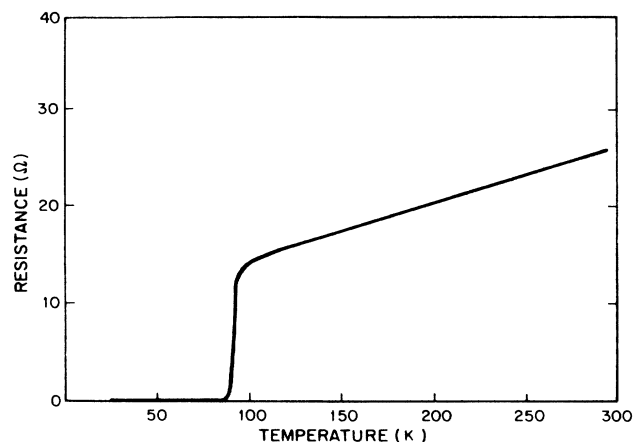

FIG. 1. A typical resistance vs temperature curve for the samples studied.

phous and highly resistive. A post growth anneal in oxygen at about 870 °C for 1 h made the films superconducting with an onset above 94 K and zero resistance in the range 80–85 K. A typical resistance as a function of temperature curve is shown in Fig. 1. X-ray diffraction indicated that these films are orthorhombic, polycrystalline without a significant degree of preferred orientation. Energy-dispersive elemental analysis in a scanning electron microscope showed that the composition of the films was close to the stoichiometric 1:2:3 composition.

The design of the CSTM used in these experiments is based on the design of LeDuc et al.[9] Details will be published elsewhere.[10] CSTM tips used were cleaved from platinum wire or fashioned from thin niobium sheets. Tips made from gold or lead were unable to penetrate the oxide layer to form junctions. The CSTM is mounted on the end of a dewar probe. The entire assembly is inserted into a liquid helium dewar resting on a vibration isolation table.

The CSTM is operated in the constant feedback mode.[9] An adjustable amplitude ac voltage sweep (∼13 Hz) is applied to the sample while a fixed-amplitude voltage sweep of the same frequency references a lockin amplifier (LIA). The tip senses a current signal of this frequency that is detected and amplified by a field effect transistor (FET) op-amp package located at the top of the dewar probe. This signal is then nulled and sent into the LIA. The LIA is operated so that a current signal of a given amplitude produces a constant output voltage. If the tunneling resistance changes, the LIA output voltage will vary such that the current signal amplitude is constant. The output voltage is amplified and fed-back to the piezo element controlling the tip-sample separation. The response of the system is determined by the adjustable time constant of the LIA.

The resulting I-V curves are monitored on an oscilloscope and can be videotaped. The current signal can also be time averaged with a signal averager. We note that the purpose of the averager is only to eliminate high-frequency noise from the signals. Data obtained in this way are stored in a laboratory computer. Further details of the electronic and data acquisition system will appear later.[10]

III. RESULTS AND DISCUSSION

A. Current notch

Our instrument has been successful in measuring the energy gap of classic superconductors lead and niobium. These preliminary measurements were performed to test the CSTM and the feedback and data acquisition electronics. Figure 2 shows an example where a crashed gold tip has picked up a coating of lead from a bulk lead sample forming a superconductor-insulator-superconductor tunnel junction. The I-V curve shows the dual gap of the expected size and shape; the conductance exhibits the distinctive dip in the density of states at zero bias.

Initial results on bulk YBa₂Cu₃O₇ were very dependent on tip placement on the sample in the x, y, and z directions. I-V curves obtained from the bulk samples were rarely repeatable. However, the thin-film samples described above produced very repeatable data which appears characteristic for this type of sample. Figure 3 shows a typical curve measured for the thin films. The distinctive feature is a linear, high-conductance current step, or current notch, at zero bias. In the majority of cases, the notch was symmetric about zero bias although small (< 10 mV) shifts along the voltage axis were observed. Note that the conductance shape for this current notch is very near the mathematical inverse of the conductance of the lead-lead junction. This data indicates a build up in the density of states at zero bias rather than a dip seen for the lead. Curves of this type were found for a wide range of tunneling resistances ($R_t \sim 10^6 - 10^9 \Omega$) on different samples and different positions on the same sample. Positions on the same sample were changed macroscopically on the order of microns to millimeters (warm-
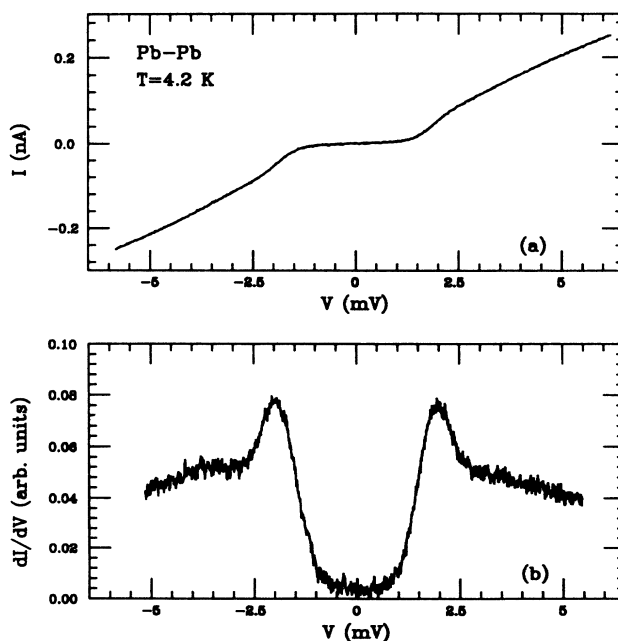

FIG. 2. (a) I-V characteristic of a lead-lead junction formed between a lead-coated gold STM tip and bulk lead. (b) Digitally calculated conductance curve for the I-V data of (a). The characteristic dip in the conductance of a superconductor-insulator-superconductor tunnel junction at zero bias is evident.
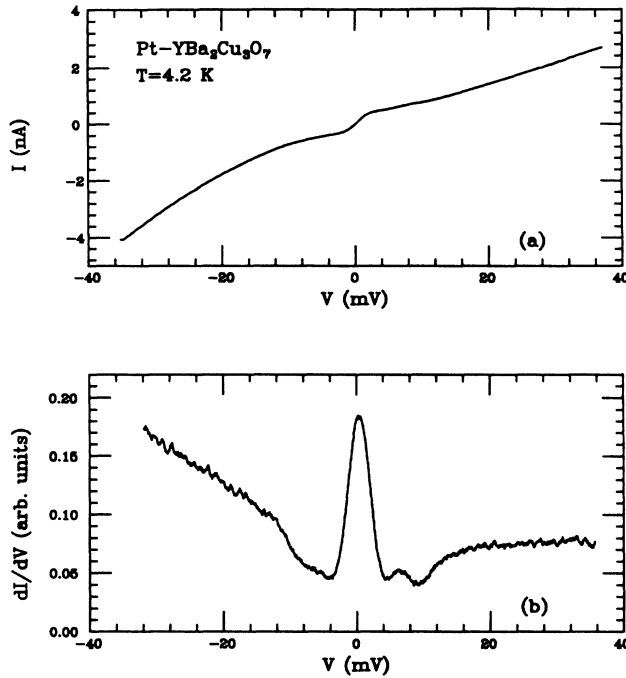
FIG. 3. (a) I-V characteristic showing the current notch at zero bias. (b) Digitally calculated conductance for the I-V data of (a). Note the striking increase in the conductance at zero bias. This data is characteristic for the thin-film (thickness ~ 2 μm) $YBa_aCu_3O_7$ studied. Most likely, the large conductance at zero bias is related to Josephson effects within the films.
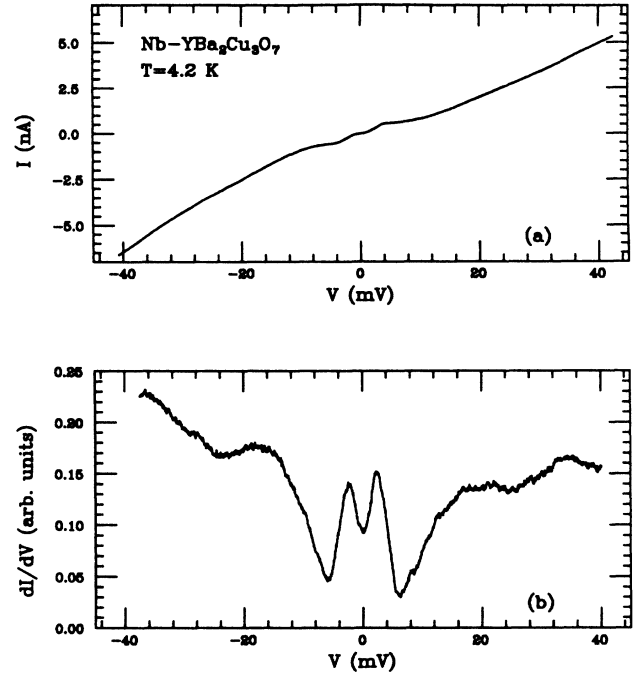
FIG. 4. (a) An I-V curve taken using a superconducting niobium STM tip, the niobium gap is observed within the notch at zero bias. (b) Digitally calculated conductance curve for the I-V data of (a). The conductance shows the gap to be about the size expected for niobium. The fact that the niobium gap is visible indicates that tunneling largely contributes to the observed current.

ing up the CSTM at the top of the dewar and reapproaching after cooling or moving the sample on the sample holder) and microscopically on the order of angstroms (moving the sample with a translation piezo). In addition, this I-V characteristic was found for samples prepared on different substrates. The majority of the samples studied were on sapphire substrates; however similar samples on $SrTiO_3$ were also studied with identical results. The width of the conductance peak varied somewhat between 7 to 12 mV and the current step height varied approximately linearly with $1/R_t$.

The use of a niobium STM tip was motivated by the possibility of observing the sum of the niobium and $YBa_2Cu_3O_7$ gap. Figure 4 shows a typical I-V curve taken with a niobium tip on one of the same samples showing the simple notch when probed with a platinum tip. The I-V characteristic now shows the gap of niobium within the current notch. The ability to observe and measure the niobium gap indicates that all or most of the current is from tunneling electrons. This is not surprising given the large resistances of the point contacts.

Although the current notch feature was characteristic of a large majority of data, and remarkably reproducible, it is the least understood of the phenomena observed in this study.

Recent experiments on current biased, lithographically fabricated two-dimensional (2D) arrays of small capacitance $(C \sim 10^{-15})$ Josephson junctions[11] show an I-V curve very similar to our current notch characteristic for

low normal-state resistance (R_N) arrays. The amplitude of the notch feature of these arrays, as with our data, was inversely proportional to R_N. However, the conductance of the array notch was much steeper than our notch conductance. The geometry of our experiment could lend itself to a junction array picture. The CSTM tip is generally about a centimeter or so away from the ohmic contact with the sample. Assuming a grain size of about 1 μm, this yields about 10^4 junctions between the tip and ohmic contact driven by the high-impedance junction formed at the STM tip. This high-impedance junction could be thought of as an effective current source for the array of junctions within the thin-film sample. (Presumably, the I-V curve measured directly between two ohmic contacts on the sample would be somehow different from the current notch.[12]) The lower conductance at zero bias in our experiment could be due to the proposed array having resistive components along its length. The magnitude of the zero-bias conductance varied somewhat for different tip positions; this would be the expected behavior if the number of resistive components changed in the array. Direct comparison between our experiment and the 2D array experiment is problematic. Detailed characterization of the intergrain geometry of the thin films is difficult and the precise nature of the 2D array measurements is unclear. Nevertheless, the qualitative similarity between our current notch curves and the low-impedance array characteristics suggests our experiment may observe similar phenomena. Notchlike characteristics have

also been observed in low-impedance (~ 100 Ω), current driven point contact junctions between a niobium probe and a bulk YBa$_2$Cu$_3$O$_7$ sample;[13] this experiment directly observed ac and dc Josephson effects.

The fact that models assuming the intergrain junctions to be Josephson junctions have been used successfully in analyzing other experimental data involving high T_c superconductors has lead our thoughts concerning our data in this direction. Work measuring the I-V curves of grain boundaries in thin films[12] show characteristic resembling the tunneling characteristics between superconductors with a low Stewart-McCumber parameter, β.[14,15] (This parameter determines the amount of hysteresis one expects in a Josephson junction I-V characteristic, $\beta \sim I_c R_N^2 C$, where I_c is the junction's critical current, R_N is the normal state resistance, and C is the capacitance.) Models invoking intergrain Josephson coupling have been used to explain, among other things, transport properties in bulk materials[16] and rf loss in thin films[17] of 1:2:3 superconductors. These models have been in reasonable agreement with experiment.

Recently, Hess et al.[18] have measured the I-V characteristics at a vortex core using an STM to probe the core. Their experiments show a peak in the differential conductance (dI/dV) or in the local density of states (DOS) which is very similar to the conductance shown in Fig. 3(b). It is possible that similar mechanisms can explain both observations. Overhauser and Daemen[19] proposed a simple model to account for the observations of Hess et al. According to their approach, the peak in the conductance is attributed to self-energy corrections of the normal electrons in the core caused by coupling (via second order perturbation, see also Ref. 20) to the superconductor excitations outside the core. The stoichiometric profile of bulk single crystal YBa$_2$Cu$_3$O$_7$ has shown that surface chemical composition can be much different than the bulk.[21] The surface properties of our films have not been characterized but it is feasible that their surface structure is such that we probe a normal layer coupled to the underlying superconducting films in a way leading to a mechanism like the one outlined above. The overall voltage width of the current notch remained fairly constant while the current height varied proportionally to $1/R_t$. This would be the expected behavior of the voltage width according to this interpretation, but it is not clear what would be expected from the current height. It is possible that the varying STM tip pressure by tip movement in the z axis changes the coupling and thus the current amplitude of the notch. From this interpretation, the superconducting energy gap for our samples would be 3.5-6.0 mV, on the low end of values published to date. It could be that this effect is responsible for the finite slope of the notch while the overall shape of the notch characteristics is due to Josephson effects.

Lastly, we briefly consider superconducting proximity effects. Structures consisting of a normal metal sandwiched between two identical superconductors can support a supercurrent through the system,[22] given that the thickness of the normal metal is not too thick with respect to the coherence length of the superconductor.

This effect was used in tunneling structures[23] to determine the properties of superconductors that did not lend themselves easily to producing conventional tunnel junctions. The structures consisted of the superconductor under study in intimate contact with a thin (thickness ≤ 100 Å) normal metal that readily formed a tunneling barrier; atop this was evaporated a counter-electrode, forming a tunnel junction between the normal metal and the counterelectrode. The I-V characteristics for the junction were very nearly what would be expected for the superconductor from BCS theory, showing the characteristic conductance dip near zero bias.[24] The proximity of the superconductor yields normal metal electronic properties almost identical to a superconductor. While it is easy to conceive possible arrangements of the STM tip–normal region-superconducting region forming structures where proximity effects could be important, it seems unlikely that these effects would result in an increase in the conductance at zero bias. Therefore, proximity effects appear to play no role in the current notch phenomena.

B. Charging steps

It is predicted[25,26] that for two ultrasmall tunnel junction connected in series, a low-conductance region near zero bias will be observed (the Coulomb blockade), and for certain junction parameters, steps will appear in the I-V characteristic. In particular, when the tunneling rate and resistance of one of the junctions is much different from the second, current steps appear corresponding to the average number of excess electrons on the shared electrode. This effect has been experimentally observed by some of us[27] with the CSTM system described. In that experiment, small (~ 100 Å diameter) indium droplets were evaporated on a thin, continuous film of aluminum. The droplets were then probed with the CSTM tip to produce the two ultrasmall (capacitance $\sim 10^{-18}$ F) junctions in series. One junction was formed between the tip and droplet, the other between droplet and the oxidized aluminum substrate. The quality of the steps observed allowed us to make a quantitative comparison with a stochastic theory of the tunneling process.[26] Other groups using a CSTM have observed this effect on aluminum droplets[28] and in lead films.[29] The latter showing, among other things, superconducting gap effects in addition to the Coulomb blockade and current steps.

Some of the earlier tunneling experiments on high T_c superconductor revealed what some thought to be "multiple gaps."[30,31,32] It was soon realized[33,34] that this phenomena could be explained theoretically assuming a two junction system. For instance, if one assumes that an electron tunnels from an electrode (like an STM tip) to an isolated superconducting grain then to the bulk, a two junction system like that described above giving rise to steps in the I-V characteristics could be realized.

Such steps were often observed in our study of thin-film samples; an example of these I-V characteristics is curve A of Fig. 5. As in our previous work,[27] we analyze the data by comparing the experimental I-V characteristic to a theoretical curve produced using the semiclassical model of small tunnel junctions.[35,36] The method used to

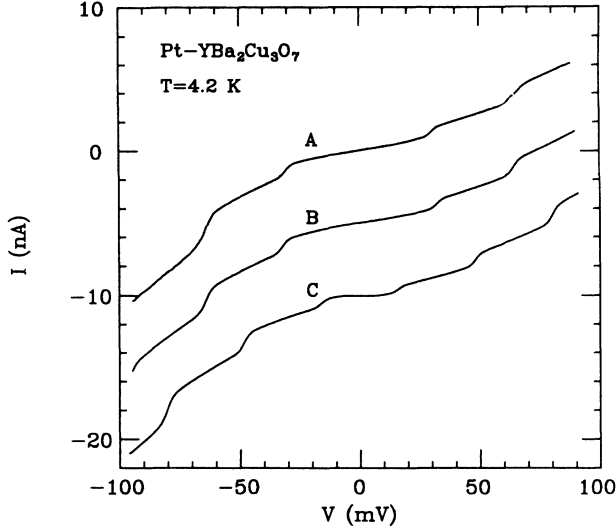WILKINS, AMMAN, SOLTIS, BEN-JACOB, AND JAKLEVIC

FIG. 5. Curve A is an experimental I-V characteristic showing prominent capacitive charging steps. Offset for clarity, curve B is a theoretical fit to the data for $C_T = 5 \times 10^{-18}$ F, $C_G = 1.2 \times 10^{-17}$ F, $R_T = 3.1 \times 10^7$ Ω, and $R_G = 1 \times 10^3$ Ω. The fit requires a voltage shift of 16 mV ($V_P = 4.7$ mV) and curve C is calculated for $V_P = 0$. The asymmetry in the prefactor α is about a factor of two, the lower value is $17 V^{-1}$. Junction parameters and the prefactor α are defined in the text.

calculate the curve B of Fig. 5 involved the solution of the appropriate master equation[37] while in Ref. 27 a stochastic method[26] was used to obtain the theoretical fits; the two methods give the same results. In interpreting the data, we assume a STM tip-isolated grain-bulk configuration to make the two tunnel junction system. The capacitances and resistance of the two tunnel junctions are labeled C_T and R_T for the tip-grain junction and C_G and R_G for the grain-bulk junction. The middle theoretical curve of Fig. 5 is fit by measuring the magnitude of features of the data. For example, the capacitance corresponding to the larger resistance is determined by the voltage width of the current steps: $\Delta V_{\text{step}} = e / C_T$, where e is the fundamental charge unit.

Curve C of Fig. 5 shows a theoretical plot with the fitted junction parameters when the junction voltages are determined solely by the external applied voltage, the number of surplus electrons on the grain, and the capacitances of the tunnel junctions. The Coulomb blockade region is symmetric about zero bias. Typically, experimental data (like the experimental I-V characteristic of Fig. 5) does not display this simple behavior. There is an added contribution to the junction voltages, called V_P, exhibited in the data as a voltage shift V_S, where $V_S = V_P(C_G + C_T)/C_T$. When this shift is close to the half-step width, the step closest to zero bias has a very small height and the Coulomb blockade region appears to have twice the expected width. Such is the case with the data shown in the curve A of Fig. 5. In Ref. 27 we attributed this shift to residual polarization in the aluminum oxide near a droplet (also described in Ref. 29). We assume that a similar polarization in the vicinity of the grain is responsible for the shift observed in this experiment. Curve B of Fig. 5 contains no superconducting energy gap. Our theoretical work, assuming a simple BCS density of states for the superconductor and only tunneling current, indicates that an energy gap cannot account for the extra wide region about zero bias. The magnitude of the conductance at zero bias cannot be modeled assuming an energy gap at 4 K.

If only a constant DOS and an energy independent tunneling matrix element are assumed, the envelope of the charging steps should be linear with slope $R = R_T + R_G$. This is clearly not the case in the experimental I-V characteristic whose envelope rises faster than linear. Many effects (Ref. 1, and references therein) can produce nonlinear behavior in the I-V characteristics of tunnel junctions. As a first approximation, we have accounted for the nonlinearity by phenomenologically adding a quadratic ($\alpha V^2/R$) term to the tunneling rates of each junction. The prefactor α is determined from the observed variation of the step height. To fit the data shown, it was necessary to use a different α for one of the tunneling rates. The step heights on the positive-bias side of the characteristic are changing less dramatically than on the negative-bias side. This behavior is reminiscent of the asymmetric nature of Schottky barrier junctions (Ref. 1, and references therein) and may be a result of a semiconductorlike oxide on the surface of the films. Asymmetries of other types where found for I-V characteristics having charge steps. For example, in one case, the I-V characteristic showed clear, symmetric ($V_P = 0$) steps except the first step on one side was twice the expected height. Nonideal behavior was also observed in the indium droplet experiment but with much less frequency than with these thin films, indicating that the films are a much more complicated and less easily characterized system.

Finally, we would like to point out that the data presented here represents a different regime of the tunneling parameters than the regime in which the indium droplet experiment operated. In that experiment, both the capacitances and resistances of one junction were greater than the other, producing very sharp steps. In the present experiment, the larger capacitance corresponds to the smaller resistance and is larger only by a factor of about two from the lower capacitance. Yet clear steps are still possible because $R_T \gg R_G$.[26] Intuitively, the relative magnitude of the capacitances and resistances are consistent. The STM generally operates with tunneling resistances from 1 to 100 MΩ and the grain is somehow embedded in the bulk. The smaller tip capacitance is not surprising given an expected larger tip to grain distance (compared to expected average grain to bulk distances) and possible curvature of the tip effects. (This is in contrast to the indium droplet experiment where we found the tip to droplet capacitance the larger capacitance.)

C. Negative differential resistance

The most unusual I-V characteristics observed from these samples were those exhibiting negative differential
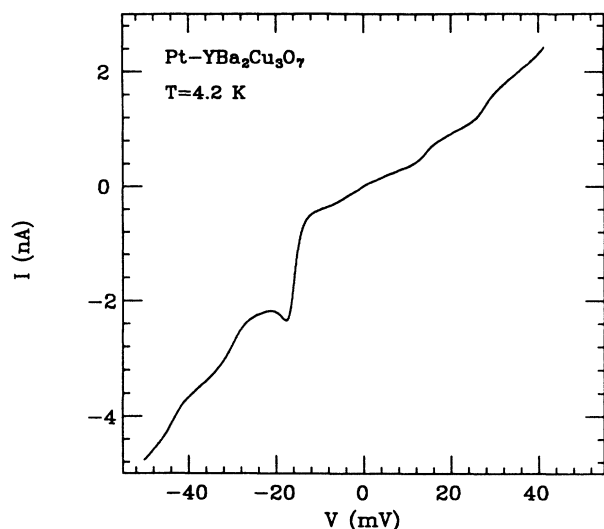
FIG. 6. I-V characteristic showing negative differential resistance (NDR). Characteristics like these were seen on several of the samples studied. The appearance of NDR in the I-V characteristic depended greatly on STM tip position.

resistance (NDR) such at the I-V shown in Fig. 6. Characteristics with NDR were highly asymmetric with the NDR appearing only on one side of the curve at any one time. This is a true NDR: the voltage sweep could be offset so that the junction could be biased in the region of negative resistance. Most occurrences of NDR were with the sample at negative bias. All these curves had the same general shape of Fig. 6 with the current dip at roughly the same voltage in each case (~ 20 mV). This type of NDR was observed for both platinum and niobium tips and on different samples. In both cases the structure at zero bias (notch, notch plus gap) was present but washed out somewhat. The washing out may be due to the relatively low tunneling resistances of the junctions with NDR (none higher than about 10^7 Ω). The presence of NDR did not exclude charging steps from the measured I-V characteristics. Figure 6 clearly shows steps in the curve at large voltages. We cannot say that the charging steps are fundamentally associated with the NDR; however, we also observed NDR in the experiment with the indium droplet samples described above.[27] Our efforts to model NDR assuming multidroplet tunneling or interdroplet tunneling failed to yield any system exhibiting NDR. Moving the tip in the sample area where NDR occurred generally produced highly nonlinear, unstable and unrepeatable curves.

Two devices that are known to display NDR in their I-V characteristics are quantum-well structures and the Esaki diode. Quantum-well structures exhibit NDR resulting from resonant tunneling through quantized states of the well.[38] Assuming a narrow range of k values for the tunneling electrons, one could visualize a double barrier forming between tip-grain-bulk as in the charging step cases, or between adjacent grains. The energy of the level indicated here would correspond to a quantum box ~ 250 Å wide, much smaller than the expected grain size.

(Interestingly, this is the order of the grain size one would expect from the voltage width of typical charging steps observed for these samples.) However, depending on the geometry of the probed grain, states could be quantized in a particular direction allowing resonant tunneling in this direction.[39] In contrast to our results, quantum-well devices have regions of NDR at both positive and negative voltages and are fairly symmetric about zero bias. The second device, the Esaki diode, consists of the junction between two regions of highly and oppositely doped semiconductor.[40] NDR is observed in the forward bias direction. It is possible in this experiment that the tip is probing the interaction of two regions in the semiconductor-like oxide layer containing different impurities, thus forming a local Esaki diode structure. An alternative explanation is based on the work of Lyo and Avouris;[41] very recently, these authors observed NDR with a room temperature STM on samples of boron-exposed silicon (111). The sample was topographically characterized and sites with boron impurities identified. Spectroscopy performed on these impurity sites could exhibit NDR. The types of I-V curves observed show striking qualitative resemblance to our tunneling spectra. Using a model assuming localized states for both the tip and the sample ("localized quasiatomic states") density of states, Lyo and Avouris simulate their I-V characteristics with good qualitative agreement. Since the NDR in our experiment is asymmetric, we think it likely that the results stem from one of the latter two mechanism discussed. Further, the very suggestive resemblance between our data and the results of Lyo and Avouris indicates that the two experiments may be observing similar effects. Namely, our experiment may probe localized states in the surface layer of the thin-film sample. In support of this, for a particularly stable instance of NDR, we were able to dial the NDR in and out of the I-V curve by changing the overall junction resistance. This was accomplished by moving the embedded tip vertically in the oxide layer, probing different regions within the layer. This procedure is expected to be analogous to Lyo and Avouris scanning a boron impurity site on the silicon surface.

D. Energy gap

Finally we would like to comment on the superconducting energy gap. Many groups using different techniques have reported tunneling spectroscopy data with gaplike features (for a recent review see Ref. 42). For the case of point contact-type experiments using an STM, such as ours, gaplike I-V characteristics were often found only after repeatedly driving the STM tip into the sample. This process presumably allows the tip to expose the bulk superconductor, letting the gap be revealed in the tunneling spectra. Since it was not necessarily the intent of this experiment to measure the energy gap, we made careful approaches with the STM tip to the sample and, using a long time constant on the LIA in the feedback circuit, gently penetrated the oxide layer. This method most often gave the notch I-V characteristics. However, we also had a few instances where the data could be
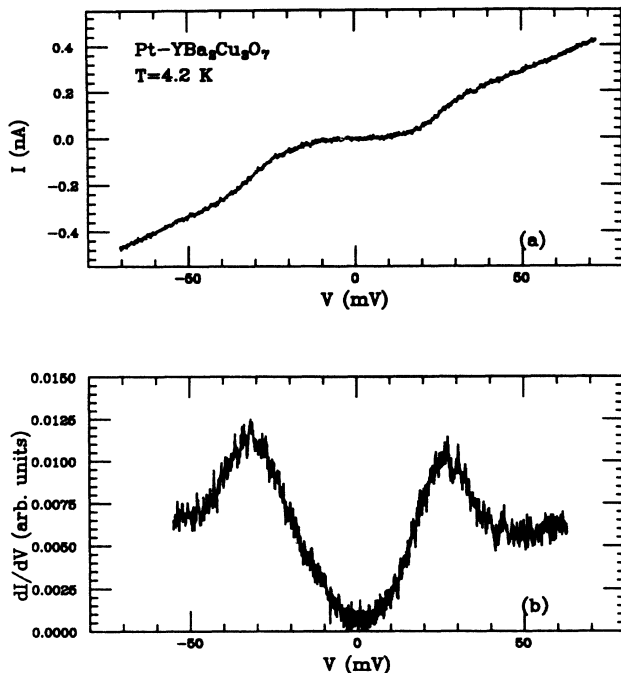
FIG. 7. (a) I-V characteristic and (b) digitally calculated conductance curve for thin film $YBa_2Cu_3O_7$ probed with a platinum STM tip showing energy gaplike behavior.

called gaplike; the best is shown in Fig. 7, having a gap value of about 27 mV. We find values for the gap based on this selected data range from 6 to the 27 mV of Fig. 7, within the range of values one finds in the literature. Consistent with other experiments, most of our "gap" data were found in spots where the tip had been crashed into the sample or dragged through the oxide by the scanning piezo. Concerns that some I-V data apparently showing gaps could actually be due to charge effects may have some validity: some of our data with gaplike features have faint charge steplike structure at large voltages and are often associated with a location on the sample showing clear charging steps. In addition, at voltages above the gap, the data tends to be highly nonlinear. This is in contrast to the I-V characteristic of Fig. 7 which shows a tendency toward an ohmic limit at voltages beyond the gaplike one would expect of a BCS superconductor (compare to Fig. 2). We raise this point because some of our gaplike data resemble data observed by some of us in the indium droplet experiment; data where the charging steps were not clear or simply showed a Coulomb blockade. Because of this ambiguity, we feel care must be taken in interpreting results from point contact experiments on high-T_c superconductors.

*Also at The School of Physics and Astronomy, Raymond and Beverly Sackler Faculty of Exact Sciences, Tel Aviv University, 69978 Tel Aviv, Israel.

[1] E. L. Wolf, in *Principles of Electron Tunneling Spectroscopy* (Oxford University Press, New York, 1985).

[2] J. R. Kirtly, C. C. Tsuei, Sung I. Park, C. C. Chi, J. Rosen, and M. Shafer, Phys. Rev. B 35, 7216 (1987).

[3] S. Pan, K. W. Ng, A. L. de Lozanne, J. M. Tarascon, and L. H. Greene, Phys. Rev. B 35, 7220 (1987).

[4] J. Moreland, J. W. Ekin, L. F. Goodrich, T. E. Capobianco, A. F. Clark, J. Kwo, M. Hong, and S. H. Liou, Phys. Rev. B 35, 8856 (1987).

[5] A. Fournel, I. Oujia, J. P. Sorbier, H. Noel, J. C. Levet, M. Potel, and P. Gougeon, Europhys. Lett. 6, 653 (1988).

[6] J. Geerk, X. X. Xi, and G. Linker, Z. Phys. B 73, 329 (1988).

[7] M. Gurvitch, J. M. Valles, Jr., A. M. Cucolo, R. C. Dynes, J. P. Garno, L. F. Schneemeyer, and J. V. Waszczak, Phys. Rev. Lett. 63, 1008 (1989).

[8] M. Aslam, R. E. Soltis, E. M. Logothetis, R. Ager, M. Mikkor, W. Win, J. T. Chen, and L. E. Wenger, Appl. Phys. Lett. 53, 153 (1988).

[9] H. G. LeDuc, W. J. Kaiser, and J. A. Stern, Appl. Phys. Lett. 50, 1921 (1987).

[10] R. Wilkins and R. C. Jaklevic (unpublished).

[11] L. J. Geerligs and J. E. Mooij, Physica 152B, 212 (1988).

[12] P. Chaudhari, J. Mannhart, D. Dimos, C. C. Tsuei, J. Chi, M. M. Oprysko, and M. Scheuermann, Phys. Rev. Lett. 60, 1653 (1988).

[13] J. Kuznik, M. Odelnal, S. Safrata, and J. Endal, J. Low Temp. Phys. 69, 313 (1987).

[14] W. C. Stewart, Appl. Phys. Lett. 12, 277 (1968).

[15] D. E. McCumber, J. Appl. Phys. 39, 3113 (1968).

[16] R. L. Perterson and J. W. Elkin, Phys. Rev. B 37, 9848 (1988).

[17] T. L. Hylton, A. Kapitulnik, M. R. Beasley, John P. Carini, L. Drabeck, and George Gruner, Appl. Phys. Lett. 53, 1343 (1988).

[18] H. F. Hess, R. B. Robinson, R. C. Dynes, J. M. Valles, Jr., and J. V. Waszczak, Phys. Rev. Lett. 62, 214 (1989).

[19] A. W. Overhauser and L. L. Daemen, Phys. Rev. Lett. 62, 1691 (1989); An alternate calculation of the vortex DOS peak based on a solution to the Bogoliubov-de Gennes equations is given by J. D. Shore, M. Huang, A. T. Dorsey, and J. P. Sethna, Phys. Rev. Lett. 62, 3089 (1989).

[20] A. W. Overhauser, Appl. Phys. Lett. 54, 2490 (1989).

[21] Z. Z. Wang, B. Y. Lin, A. Kahn, and N. P. Ong, Bull. Am. Phys. Soc. 34, 423 (1989).

[22] J. Clarke, Proc. Roy. Soc. London, Ser. A 308, 447 (1969).

[23] E. L. Wolf and G. B. Arnold, Phys. Rep. 91, 31 (1982).

[24]E. L. Wolf, J. Zasadzinski, J. W. Osmun, and G. B. Arnold, J. Low Temp. Phys. **40**, 19 (1980).

[25]I. O. Kulik and R. I. Shekhter, Zh. Eksp. Teor. Fiz. **68**, 623 (1975) [Sov. Phys.—JETP **41**, 308 (1975)].

[26]K. Mullen, E. Ben-Jacob, R. C. Jaklevic, and Z. Schuss, Phys. Rev. B **37**, 98 (1988).

[27]R. Wilkins, E. Ben-Jacob, and R. C. Jaklevic, Phys. Rev. Lett. **63**, 801 (1989).

[28]P. J. M. van Bentum, R. T. M. Smokers, and H. van Kempen, Phys. Rev. Lett. **60**, 2543 (1988).

[29]K. A. McGreer, J.-C. Wan, N. Anand, and A. M. Goldman, Phys. Rev. B **39**, 12 260 (1989).

[30]I. Iguchi, H. Watanabe, Y. Kasai, T. Mochiku, A. Sugishita, and E. Yamaka, Jpn. J. Appl. Phys. **26**, L645 (1987).

[31]J. Moreland, L. F. Goodrich, J. W. Elkin, T. E. Capobianco, and A. F. Clark, Jpn. J. Appl. Phys. **26**, Suppl. 26–3, 999 (1987).

[32]J. R. Kirtley, C. C. Tsuei, S. P. Park, C. C. Chi, J. Rosen, M.

W. Shafer, W. J. Gallagher, R. I. Sandstrom, T. R. Dinger, and D. A. Chance, Jpn. J. Appl. Phys. **26**, Suppl. 26–3, 997 (1987).

[33]S. T. Ruggiero and J. B. Barner, Phys. Rev. B **36**, 8870 (1987).

[34]K. Mullen, E. Ben-Jacob, and S. Ruggiero, Phys. Rev. B **38**, 5150 (1988).

[35]E. Ben-Jacob, Y. Gefen, K. Mullen, and Z. Schuss, Phys. Rev. B **37**, 7400 (1988).

[36]K. K. Likharev, IBM J. Res. Dev. **32**, 144 (1988).

[37]M. Amman, K. Mullen, and E. Ben-Jacob, J. Appl. Phys. **65**, 339 (1989).

[38]L. L. Chang, L. Esaki, and R. Tsu, Appl. Phys. Lett. **24**, 593 (1974).

[39]R. C. Jaklevic and John Lambe, Phys. Rev. B **12**, 4146 (1975).

[40]L. Esaki, Phys. Rev. **109**, 603 (1958).

[41]In-Whan Lyo and Phaedon Avouris, Science **245**, 1369 (1989).

[42]J. R. Kirtley, Int. J. Mod. Phys. B (to be published).